(A2) and the value of a_D in Eq. (A3) is assumed to be equal to the value of the corresponding parameter in the nonlocal potential. The resulting local potential $U_L(r)$, modified by the addition of a spin-orbit term, is used as described in Sec. IV.B.1 to calculate the various optical-model cross sections. The approximation (A3) is particularly convenient since it can be used without modification in existing optical-model computer programs. In Fig. 12, the equivalent local potential determined by substituting approximation (A3) in Eq. (A1) is compared with the nonlocal potential given by Eq. (A2).

For those cases for which all requisite calculations were made, the values of the differential cross section and polarization calculated by use of the approximation (A3) agreed slightly better with the predictions of the actual nonlocal model of Ref. 14 than did values calculated directly by use of Eq. (A1). In fact the differences between calculations based on Eq. (A3) and those based on the nonlocal model of Perey and Buck were small enough that they might reasonably be ascribed to differences in numerical routines in the two computer codes. The differential cross sections and polarizations calculated by these methods are compared in Fig. 13.

As far as agreement with the observed data is concerned, it seems reasonable to think of Eqs. (A1) and (A3) as constituting a "model" quite independent of their relation to the original nonlocal model. However, the results described in the previous paragraph indicate that such a distinction is not necessary and, in particular, that Eq. (A3) is an adequate approximation to an equivalent local potential for the ranges of energy and mass number of concern here.

PHYSICAL REVIEW VOLUME 133, NUMBER 1B 13 JANUARY 1964

Average Energy and Angular Momentum Removed from Dy Compound Nuclei by Neutrons and Photons*

JOHN M. ALEXANDER† AND GABRIEL N. SIMONOFF‡
Lawrence Radiation Laboratory, University of California, Berkeley, California
(Received 7 June 1963)

Excitation functions are presented for many heavy-ion-induced (HI) reactions that produce Dy^{149}, Dy^{150}, and Dy^{151}. Projectiles were C^{12}, N^{14}, N^{15}, O^{16}, O^{18}, F^{19}, Ne^{20}, and Ne^{22} of 4 to 10.4 MeV per amu. The reactions studied are all of the type (HI,xn), where x ranges from 3 to 11. A large fraction of the total reaction cross section is accounted for by these (HI,xn) reactions—0.9 at approximately 45 MeV to 0.4 at approximately 120 MeV. An analysis to obtain the energy of the first emitted neutron is presented. Comparison of the results of this analysis to angular-distribution studies suggests that the first neutron removes 2 to 4$\hbar$ units of angular momentum. We obtain the relationship between average total photon energy and average angular momentum removed by photons. Comparison with the average individual photon energy from other work leads to an average of $1.8\pm0.6\hbar$ for the angular momentum removed by each photon. The excitation energy E_j of the lowest lying state of spin J has been estimated.

I. INTRODUCTION

CURRENTLY available beams of heavy ions (HI) make it possible to study compound nuclei over a wide range of excitation energy and angular momentum. Radiochemical studies are quite useful because they give information about specific reactions; e.g., the (HI,5n) reaction can be studied without interference from the reactions (HI,6n), (HI,$p5n$), etc. This specificity is difficult to obtain by physical means because of complex coincidence-detection requirements. The products Tb^{149g}, Dy^{150}, and Dy^{151} have been extensively studied because they can be easily identified by their characteristic alpha radioactivity.

In previous studies we have presented recoil-range data that give strong evidence that these products are produced by essentially pure compound-nucleus reactions.[1–3] Also reported are angular-distribution measurements from which it has been possible to obtain the average total energies (T_n and T_γ) of neutrons and photons.[3]

The experimental data reported here consist of excitation functions for 36 reactions of type (HI,xn)Dy^{149}, (HI,xn)Dy^{150}, (HI,xn)Dy^{151}. Compound nuclei of masses 154 to 160 have been formed by various projectiles and targets.

The conventional treatment of excitation-function data involves the use of the statistical model with little, if any, allowance for the effect of angular momentum. This type of treatment may possibly be

* Work done under the auspices of the U. S. Atomic Energy Commission.
† Present address: Department of Chemistry, State University of New York at Stony Brook, Stony Brook, New York.
‡ Present address: Nouvelle Faculté des Sciences de Bordeaux, Talence (Gironde) France.

[1] L. Winsberg and J. M. Alexander, Phys. Rev. **121**, 518, 529 (1961).
[2] J. M. Alexander and D. H. Sisson, Phys. Rev. **128**, 2288 (1962).
[3] G. N. Simonoff and J. M. Alexander, following paper, Phys. Rev. **133**, B104 (1964).

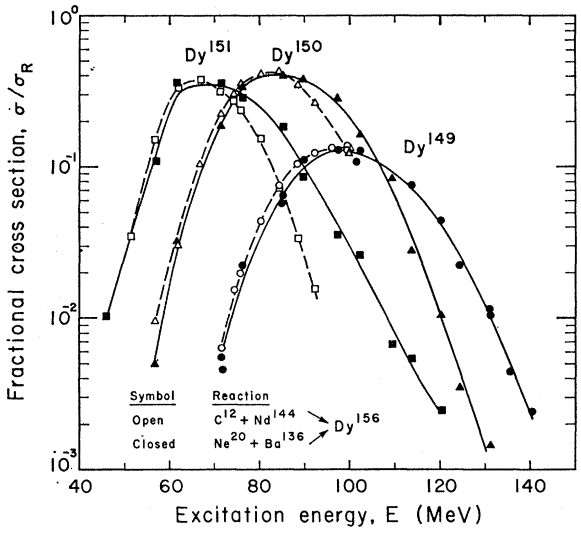

FIG. 1. Measured cross section σ divided by calculated total reaction cross section σ_R as a function of excitation energy E.

acceptable for reactions induced by protons and helium ions of several tens of MeV. However, it is clearly unsatisfactory for reactions between complex nuclei that involve angular momenta of several tens of $\hbar$ units.[4]

We analyze the results to obtain the average energy associated with the first emitted neutron. Also, we have estimated the relationship between average total photon energy and average angular momentum removed by the photons. This relationship along with the average individual photon energy[5] gives the average angular momentum removed by each photon. By an approximate method we have estimated the energy E_j of the lowest level of spin J as a function of J.

II. EXPERIMENTAL PROCEDURES AND RESULTS

We have used the stacked-foil technique[6] to measure cross sections for 4.1-h Tb^{149g} (10% alpha), 7.4-min Dy^{150} (17.9% alpha), and 17.9-min Dy^{151} (6.2% alpha)[7] produced by many reactions between complex nuclei. The experimental conditions (targets, irradiations, counting techniques, etc.) have been described previously.[6]

The product atoms recoiled out of thin target layers (30 to 120 $\mu g/cm^2$) and were stopped in Al catcher foils of about 1.8 mg/cm^2. We measured gross alpha radioactivity with 2π ionization chambers. Activation of impurities in the catcher foils was found to be negligible.

Decay curves were graphically analyzed into the three components above. At the lower energies small amounts of 2.5-h Dy^{152} activity were observed. The presence of Dy^{152} prevented us from measuring the very small cross sections for Tb^{149} and Dy^{151} at lower energies. Separation of the activities of 7.4-min Dy^{150} and 17.9-min Dy^{151} by the decay analysis was usually quite clear. However, for those cases in which the initial activity of either species was dominant (ratio of approx. 10:1), the determination of the weaker component was subject to large error.

Various uncertainties have been discussed previously.[6] In this study the only additional uncertainties are those from analysis of the decay curves, and the decay properties of Dy^{150} and Dy^{151}. The half-periods and alpha-branching ratios for Dy^{150} and Dy^{151} have been measured by Macfarlane.[7] The half-periods are uncertain by approx. $\pm 3\%$ and lead to negligible error in the cross sections. The absolute uncertainties in the alpha branching ratios are not known but are probably about $\pm 10\%$.[7]

Resolution of the decay curves introduces no additional uncertainties for Dy^{149} cross sections. For those experiments in which the cross sections of Dy^{150} and Dy^{151} are approximately equal, standard errors from decay analysis are about $\pm 20\%$ for Dy^{151} and about $\pm 10\%$ for Dy^{150}. For experiments in which the ratio of these cross sections is approx. 8:1, the activity measurement for the species of higher cross section has a standard error of about $\pm 5\%$, and for the other species has a standard error of approx. $\pm 50\%$. Isotopically enriched materials were used for targets of Nd^{142}, Nd^{144}, Ce^{140}, Ba^{136}, Ba^{137}, and Ba^{138}. The isotopic composition of these materials is given in Table I. In the table we make a note of those isotopes for which corrections were applied in the calculation of the cross sections. It is important that these corrections be accurate for an analysis such as that presented in the next section.

The cross-section results are presented in Table II. In Fig. 1 we show some typical excitation functions (plotted as fractional cross section σ/σ_R against excitation energy E). This figure shows data for two sets of

TABLE I. Isotopic composition of the targets.

Target nuclide	Mass number and abundance (%) of the isotopes						
	142	*143*	*144*	*145*	*146*	*148*	*150*
Nd^{142}	97.45	1.04	0.89	0.21	0.26	0.08	0.07
Nd^{144}	0.56	0.67	97.3	0.8	0.67	<0.05	<0.05
	136		*138*		*140*		*142*
Ce^{140}	<0.01		<0.01		99.65		0.35
	130	*132*	*134*	*135*	*136*	*137*	*138*
Ba^{136}	<0.05	<0.05	<0.1	1.08	92.9	1.77[a]	4.24[a]
Ba^{137}	<0.03	<0.03	<0.05	<0.1	0.63	81.9	17.4[a]
Ba^{138}	0.02	0.02	0.05	0.15	0.26	1.45	98.04

[a] Corrections for these components were made in calculating the cross sections.

[4] J. R. Grover, Phys. Rev. **127**, 2142 (1962); **123**, 267 (1961).
[5] J. F. Mollenauer, Phys. Rev. **127**, 867 (1962).
[6] J. M. Alexander and G. N. Simonoff, Phys. Rev. **130**, 2383 (1963).
[7] R. D. Macfarlane, Lawrence Radiation Laboratory, Berkeley, 1962 (private communication). *Note added in proof.* More recent values (to be published by R. D. Macfarlane) for the decay properties of these nuclides are 7.20±0.10-min Dy^{150} (18±2% alpha) and 18.0±0.2-min Dy^{151} (5.9±0.6% alpha). All cross sections in this paper were calculated using the old values.

reactions that produce the compound nucleus Dy^{156}. The beam energies were calculated from range-energy curves of Northcliffe[8] and the initial energy of 10.38 MeV per amu. The cross sections given for Dy^{149} were measured by observation of 4.1-h Tb^{149g}. The values listed for Dy^{149} actually include any 4.1-h Tb^{149g} formed directly by (HI,pxn) reactions. Also, that fraction of the Dy^{149} that decayed to 4-min Tb^{149m} was not observed, and therefore is not included in the listed values. Our estimate is that the direct production of Tb^{149g} is negligible and that about $\frac{2}{3}$ of the Dy^{149} decays to Tb^{149m} and is not observed. The former estimate was discussed previously[3]; the latter is based on the fact that the fractional cross sections for Dy^{149} are all about $\frac{1}{3}$ those for Dy^{150}, or Dy^{151} from similar reactions (see Fig. 1). Relative values of the cross sections for Dy^{149} require only that the first estimate be correct; absolute values require a meaurement of the branching ratio of Dy^{149} to Tb^{149g}. More detailed studies of the decay properties of each of these nuclides would make the interpretation of these data more definite.

III. AN ANALYSIS TO OBTAIN THE AVERAGE ENERGY OF THE FIRST EMITTED NEUTRON

In this work we have measured excitation functions for a number of different reactions of the type (HI,xn) that lead to Dy^{149}, Dy^{150}, and Dy^{151}. Let us consider the relationship between two of these reactions that lead to the same product, say (HI,6n)Dy^{150} and (HI,5n)Dy^{150}, where target and projectile in the two reactions are different. It is clear that if atomic and mass numbers (Z and A) and excitation energy (E) were the only variables, then we could hope to unfold the energy spectrum of the first neutron emitted in the (HI,6n) reaction by comparing the two excitation functions. This unfolding process would be rather tedious and would require very accurate data; therefore, we attack the more modest goal of extracting the average energy $\langle\epsilon_1\rangle$ associated with the first emitted neutron (the average kinetic energy $\langle k_1\rangle$ of the first neutron plus the average total photon energy $\langle\gamma_1\rangle$ dissipated before emission of the second neutron). It is generally believed that the photon energy $\langle\gamma_1\rangle$ is very small.[4]

Let us define F_x as the fraction of those reactions in which no charged particle is emitted that lead to a specific product by an (HI,xn) reaction. The fraction of all reactions in which no charged particles are emitted is denoted by f_n. For various excitation energies (E) we have measured the cross section σ for a specific product, and we can calculate the total reaction cross section σ_R.[9] Therefore, we have

$$F_x(E)=\sigma/\sigma_R f_n, \tag{1}$$

and

$$\sum_{x=0}^{x_{\max}} F_x(E)=1. \tag{2}$$

[8] L. C. Northcliffe, Phys. Rev. **120**, 1744 (1960).
[9] T. D. Thomas, Phys. Rev. **116**, 703 (1959).

Now let us define the quantity $\langle E\rangle_x$, the average excitation energy associated with the reaction (HI,xn):

$$\langle E\rangle_x=\int_0^\infty (E)F_x(E)dE\Big/\int_0^\infty F_x(E)dE. \tag{3}$$

These $\langle E_x\rangle$ quantities can be obtained from experimental excitation functions if f_n can be determined.

Let us derive the relationship between $\langle E\rangle_x$ and $\langle E\rangle_{x-1}$. The distribution of energies (ϵ_1) associated with the first emitted neutron is denoted by $P(\epsilon_1)$. Neglecting the effect of angular momentum, we have

$$F_x(E)=\int_0^{\epsilon_{\max}} P(\epsilon_1)F_{x-1}(E-B_1-\epsilon_1)d\epsilon_1. \tag{4}$$

where $\epsilon_{\max}=E-\sum_{i=1}^{x} B_i$ and B_i is the separation energy of the ith neutron. Normalization of $P(\epsilon_1)$, such that $\int_0^\infty P(\epsilon_1)d\epsilon_1=1$, leads to the result

$$\int_0^\infty F_{x-1}(E)dE\approx\int_0^\infty F_x(E)dE. \tag{5}$$

Substituting Eq. (4) into Eq. (3), we obtain

$$\langle E\rangle_x=\int_0^\infty (E)\left[\int_0^{\epsilon_{\max}} P(\epsilon_1)F_{x-1}(E-B_1-\epsilon_1)d\epsilon_1\right]dE\Big/\times\int_0^\infty F_x(E)dE. \tag{6}$$

If $\epsilon_{\max}$ is large with respect to $\langle\epsilon_1\rangle$ then it can be replaced with small error, by ∞. The order in integration of Eq. (6) can be changed then, provided we assume that the energy distribution $P(\epsilon_1)$ does not vary with excitation energy over the region of interest,

$$\langle E\rangle_x=\int_0^\infty P(\epsilon_1)\left[\int_0^\infty (E)F_{x-1}(E-B_1-\epsilon_1)dE\right]d\epsilon_1\Big/\times\int_0^\infty F_x(E)dE. \tag{7}$$

The quantity in the square bracket is simply

$$(\langle E\rangle_{x-1}+B_1+\epsilon_1)\int_0^\infty F_{x-1}(E)dE.$$

Therefore, we have

$$\langle E\rangle_x=\frac{\int_0^\infty P(\epsilon_1)\left\{\left[\langle E\rangle_{x-1}+B_1+\epsilon_1\right]\int_0^\infty F_{x-1}(E)dE\right\}d\epsilon_1}{\int_0^\infty F_x(E)dE}. \tag{8}$$

Finally, Eq. (8) can be reduced to

$$\langle E\rangle_x=\langle E\rangle_{x-1}+B_1+\langle\epsilon_1\rangle. \quad (9)$$

From Eq. (9) one can determine the average energy $\langle\epsilon_1\rangle$ associated with the first neutron if Z, A, and E are the only variables. Even if the decay probability F_x depends on angular momentum as well as excitation energy, Eq. (9) may still be useful. For example, if there is a negligible change in angular momentum ΔJ_1 associated with the emission of the first neutron, then, Eq. (9) may be used if the average energies $\langle E\rangle_x$ and $\langle E\rangle_{x-1}$ are taken from reactions with essentially identical distributions in angular momentum. On the other hand, it may be possible to calculate or measure the change in angular momentum ΔJ_1 associated with the emission of the first neutron. If one knows experimentally the dependence of the $\langle E\rangle_x$ values on angular momentum, then values of $\langle E\rangle_x$ and $\langle E\rangle_{x-1}$ can be chosen corresponding to J values that differ by the ΔJ_1 associated with the first neutron. Alternatively, if one knows the average neutron energy $\langle\epsilon_1\rangle$, he may be able to obtain the change in angular momentum ΔJ_1.

In the next section we present values of f_n and $\langle E\rangle_x$ obtained from the excitation functions. We discuss the dependence of average excitation energy $\langle E\rangle_x$ on angular momentum and the significance of the application of Eq. (9).

IV. DISCUSSION

This work and previous studies[3,4,5,10] indicate the necessity for including angular-momentum effects in a meaningful analysis of cross-section data. The description of the dependence of nuclear level density on angular momentum requires two parameters[4]: (a) the nuclear moment of inertia (possibly dependent on excitation energy and angular momentum) and (b) the excitation energy (E_j) of the lowest excited state of spin J. We have not attempted to delimit these quantities by fitting calculated excitation functions to our data. Instead, we use Eq. (9) from the previous section to gain information about the first step in the evaporation chain, and we use a simple approximation to estimate E_j as a function of J.

We compare these results with average energies of the neutrons and photons obtained from angular distributions[3] and try to arrive at an energy and angular-momentum balance. Finally, we obtain a relationship between total photon energy and angular momentum removed by photons.

A. General Relationship of These Results to Other Studies

In a previous study[6] we have presented cross-section data for reactions of the type (HI,xn)Tb^{149g}. The results were compared with the data for (HI,xn)Dy reactions. These two reaction types show large differences in the magnitude of the peak cross sections. We can explain these differences by assuming that only those Tb compound systems of low spin ($<7.5\pm1.5$) contribute to the (HI,xn)Tb^{149g} reactions.[6]

Also we have compared angular-distribution measurements for the two reaction types (HI,xn)Tb^{149g} and (HI,xn)Dy^{149}, (HI,xn)Dy^{150}, (HI,xn)Dy^{151}. This comparison leads us to conclude that an increase in angular momentum leads to an increase in the average amount of energy dissipated by photon emission.[3] Additional evidence for this conclusion is given by the fact that the excitation functions for (HI,xn)Tb^{149g} reactions peak at 3 to 3.5 MeV per emitted neutron $[(E-\sum_{i=1}^{x}B_i)x^{-1}]$ compared with 5 to 6.5 MeV per emitted neutron for the (HI,xn)Dy reactions (see Fig. 2 of Ref. 6).

Mollenauer has studied the photons emitted in various nuclear reactions induced by He^4 and C^{12}.[5] His results indicate that total photon energy increases with increasing angular momentum. For all the reactions studied the average individual photon energy was between 1.0 and 1.6 MeV (1.1 MeV for Te+110-MeV C^{12} and 1.2 MeV for Ho+110-MeV C^{12}). His measurements of photon yields at 45 and 90° give evidence for quadrupole radiation in several reactions induced by C^{12}, with the notable exception of Te+110-MeV C^{12}. As shown in Sec. IV. B the (HI,xn)Dy reactions account for approx. 0.4 to 0.9 of the calculated reaction cross sections. Since these cross sections are such a substantial part of all the reactions, it is reasonable to assume that the average photon energy for (HI,xn) reactions is very nearly the same as that measured by Mollenauer.[5] Therefore, from Mollenauer's results it is reasonable to expect for (HI,xn)Dy reactions a value of 1.2 ± 0.3 MeV for the average individual photon energy.

B. The Fraction of the Reactions in Which No Charged Particle is Emitted

In Table II, cross-section data are given for reactions of the type (HI,xn)Dy. How does the probability for these reactions vary with type and energy of the projectile? We need this information to describe the quantity f_n (the fraction of the reactions in which no charged particle is emitted). We can expect that the probabilities for neutron evaporation from each of the Dy compound nuclei ($A=154$ to 160) will have very similar dependence on excitation energy (E). However, we do not know how the probability for compound-nucleus formation depends on type and energy of the projectile. The simplest assumptions that we can make are as follows: (a) the projectile type (C^{12}, N^{14}, etc.) is not important; (b) the energy dependence of f_n can be described in terms of the initial excitation energy of the compound nucleus.

We show values of f_n plotted against excitation

[10] J. R. Morton III, G. R. Choppin, and B. G. Harvey, Phys. Rev. **128**, 265 (1962).

TABLE II. Cross-section results. (Different experiments separated by dashed lines.)

E_b (lab) (MeV)	Cross section (mb) Dy^{149}	Dy^{150}	Dy^{151}
	$Nd^{142}+C^{12} \rightarrow Dy^{154}$		
116.3	109.	24.1	
112.4	172.	34.8	
108.1	230.	50.0	
103.7	331.	92.8	
99.0	408.	178.	
94.3	446.	358.	
89.3	381.	641.	16.9
84.1	234.	856.	100.
78.8	95.1	934.	178.
73.0	11.6	709.	323.
67.2		262.	445.
60.6			327.
53.9			55.7
122.9	52.5		
118.6	90.3		
114.2	146.		
110.2	224.		
85.8	297.		
80.5	141.		
	$Pr^{141}+N^{14} \rightarrow Dy^{155}$		
128.8	85.7	13.6	
122.9	151.	32.6	
116.6	218.	80.5	
110.5	266.	176.	
103.7	280.	376.	
96.7	197.	578.	40.4
89.5	83.0	642.	124.
81.3	12.3	478.	282.
72.8		126.	325.
63.8			138.
142.8	17.4		
137.2	32.7		
132.0	62.0		
126.4	119.		
120.8	179.		
108.6	309.		
137.5	34.8		
131.7	66.1		
125.7	124.5		
119.6	206.8	58.7	
113.0	289.8	153.1	
99.8	245.8	551.4	
92.0	135.7	648.3	
142.8	17.4	2.11	
134.1	45.8	5.68	
125.4	125.	24.0	
115.9	221.	87.2	
109.2	270.	205.	
102.3	235.	375.	
95.1	161.	588.	34.3
87.2	55.2	650.	155.
79.2	3.1	316.	322.
70.3		31.9	282.
60.5			37.0
	$Nd^{144}+C^{12} \rightarrow Dy^{156}$		
122.8	280.	274.	
118.8	282.		
114.5	262.	554.	34.2
110.5	214.	705.	67.7
106.1	149.	830.	142.
101.5	82.0	783.	292.
96.8	36.7	656.	437.
92.0	10.9	381.	537.
87.0	5.2	164.	591.
81.7		43.3	472.
76.3		11.8	189.
70.3			33.6
122.8	300.	290.	
95.	27.2	537.	490.
105.6	127.		
100.9	65.6		
96.0	24.4		
91.1	8.7		
	$Pr^{141}+N^{15} \rightarrow Dy^{156}$		
132.9	228.	169.	
126.4	243.	344.	
119.7	212.	538.	
113.0	148.	659.	130.
105.9	74.2	618.	327.
98.1	<13.	393.	433.
90.4		117.	489.
153.0	53.5		
147.9	87.0		
142.8	133.		

E_b (lab) (MeV)	Cross section (mb) Dy^{149}	Dy^{150}	Dy^{151}
	$Pr^{141}+N^{15} \rightarrow Dy^{156}$		
137.4	190.		
132.0	218.		
126.3	234.		
113.1	147.		
106.8	74.1		
148.5	85.3		
143.0	137.		
137.3	190.		
131.1	204.		
115.2	166.		
	$Ce^{140}+O^{16} \rightarrow Dy^{156}$		
163.0	62.5	14.8	
152.2	164.	65.8	
140.8	290.	292.	
132.6	264.	512.	
124.6	180.	645.	126.
115.7	85.5	690.	353.
106.9	12.5	361.	458.
96.6	<0.5	73.6	439.
86.2		<2.8	109.
74.7			<1.5
147.8	181.	100.	
140.2	249.	260.	
128.0	240.	612.	87.1
119.5	141.	745.	220.
110.7	47.9	651.	369.
101.3	<3.5	274.	622.
90.6		<18.3	326.
163.0	71.2	17.2	
151.7	162.	79.3	
131.4	240.	441.	47.5
113.8	51.5	497.	349.
104.2		255.	487.
93.8		17.0	331.
82.7			28.7
163.0	58.4		
155.5	120.		
148.6	222.		
141.3	270.		
133.6	252.		
126.2	211.		
118.4	127.		
	$Ba^{136}+Ne^{20} \rightarrow Dy^{156}$		
202.6	1.6	0.3	
190.2	5.6	0.7	
179.5	25.4	3.2	
167.2	92.8	22.1	5.2
154.6	220.	169.	13.3
140.8	233.	508.	63.5
126.7	96.1	607.	277.
111.2	6.1	210.	400.
94.4		3.2	70.8
202.6	1.2		
184.8	10.1	0.2	
172.3	48.4	7.3	
159.8	159.	58.9	11.4
146.4	246.	309.	50.2
131.9	181.	610.	139.
116.6	28.0	429.	364.
99.8		26.0	296.
81.8			2.3
179.6	23.0		
126.6	85.2		
111.4	5.2		
	$Ba^{137}+Ne^{20} \rightarrow Dy^{157}$		
202.7	11.3	3.0	
189.1	39.8	12.6	
175.0	117.	66.5	
160.0	147.	252.	33.5
146.7	102.	416.	121.
132.8	23.6	310.	301.
118.0		46.6	241.
101.5			17.1
202.7	10.3	2.3	
191.3	32.2	7.6	
179.4	91.7	38.9	
167.0	170.	147.	36.3
154.5	171.	391.	69.7
141.2	89.1	482.	256.
126.4	9.3	252.	387.
111.4		15.3	150.
95.0		0.5	2.2

E_b (lab) (MeV)	Cross section (mb) Dy^{149}	Dy^{150}	Dy^{151}
	$Ba^{137}+Ne^{20} \rightarrow Dy^{157}$		
191.4	30.9		
167.6	160.		
141.2	85.7		
	$Ce^{140}+O^{18} \rightarrow Dy^{158}$		
173.2	127.	168.	<24.
165.8	150.	259.	35.9
154.3	129.	459.	125.2
148.0	81.4	483.	206.8
135.0	34.1	381.	304.8
128.9	10.6	211.	410.7
119.9	<4.7	34.3	291.
110.2			90.2
99.5			5.0
	$La^{139}+F^{19} \rightarrow Dy^{158}$		
192.9	41.9	17.1	
179.6	107.	77.6	
169.9	142.	189.	
159.8	144.	351.	66.1
149.2	95.9	452.	168.
138.1	34.8	351.	353.
126.0	6.9	136.	341.
114.8		8.3	141.
101.1			4.9
192.9	40.0		
182.4	87.5		
170.8	137.		
160.7	142.		
149.7	97.6		
192.9	43.0		
183.2	86.5		
173.1	135.		
162.3	154.		
139.8	46.5		
128.8	12.1		
	$Ba^{138}+Ne^{20} \rightarrow Dy^{158}$		
187.2	114.	94.6	
171.2	152.	349.	50.3
153.8	72.4	466.	255.
140.4	13.5	243.0	400.
125.6	<5.5	26.5	211.
110.6		1.9	8.6
202.6	36.7		
188.8	95.4		
175.6	152.		
162.0	122.		
148.0	44.		
202.8	42.2		
154.8	67.1		
	$Ba^{137}+Ne^{22} \rightarrow Dy^{159}$		
204.2	88.5	129.5	18.9
177.5	60.7	330.6	178.
150.7		63.6	210.
136.6		2.3	43.6
124.5			1.8
223.5	34.6	17.1	1.6
210.1	76.8	67.5	8.3
196.2	100.	183.	58.0
183.9	79.5	280.	127.
170.9	40.9	282.	257.
157.3	6.0	129.	303.
143.7		13.8	129.
128.2			8.2
	$Ba^{138}+Ne^{22} \rightarrow Dy^{160}$		
223.3	66.7	78.9	36.2
210.1	86.7	179.	146.
196.0	66.4	257.	194.
181.9	24.6	230.	207.
168.5	5.3	91.2	90.4
154.7		10.3	6.5
140.4		0.98	
217.1	81.9	139.	
189.9	40.1	261.	156.
164.3		57.1	149.
223.3	74.9[a]	83.2[a]	
210.3	87.5	165.	49.1[a]
196.0	66.0	287.	149.
181.3	22.1	205.	229.
167.9		73.0	191.0
154.4		12.6	58.2
140.5		0.64	3.8

[a] These cross sections represent the relative values only. The beam current measurement failed for this experiment.

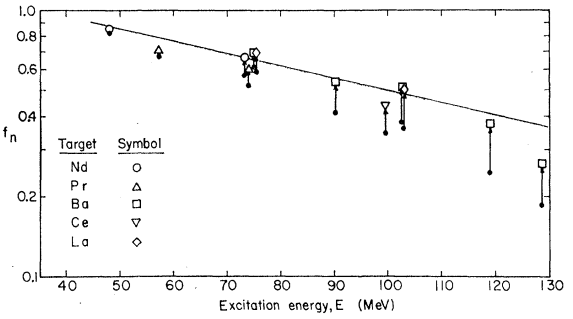

FIG. 2. The fraction f_n of the calculated total reaction cross section that leads to (HI,xn) reactions as a function of excitation energy E. The different symbols are for different target materials as shown. The arrows indicate the estimated magnitude of the contribution from reactions producing Dy^{149} and Dy^{152}. The major products are Dy^{150} and Dy^{151} (see text).

energy in Fig. 2. The values of f_n shown correspond to excitation energies for equal cross sections of Dy^{150} and Dy^{151}. At this energy we approximate f_n as

$$f_n \approx (\sigma_{151}+\sigma_{150}+8\sigma_{149}/\sigma_R), \quad (10)$$

where σ denotes cross section with numerical subscripts for the mass number of the product. The last term ($8\sigma_{149}$) in Eq. (10) is a crude estimate of the sum of the cross sections for Dy^{152} and Dy^{149}. (We estimate that the absolute cross section for Dy^{149} is three times the measured cross section; see Sec. II.) The magnitude of this term is not large as shown by the arrows in Fig. 2. The absolute values shown are uncertain by approx. $\pm 20\%$, but the relative values have standard errors of approx. $\pm 10\%$ (see Ref. 6).

We have used a single relationship for $\sigma_R/\pi R^2$ for all reactions. This relationship was obtained from the calculations by Thomas[9] for reactions of heavy ions with Pr^{141}. The values of $\sigma_R/\pi R^2$ are given in Table III, where they are compared to the sharp cutoff approximation

$$\sigma_R/\pi R^2 = 1-(V/E_{\text{c.m.}}). \quad (11)$$

The sum of the radii (radius parameter 1.5 F) of target and projectile is denoted by R, Coulomb barrier by V, and center-of-mass energy by $E_{\text{c.m.}}$. The energy dependence of σ_R from Eq. (11) and from square-well calculations is very similar for $E_{\text{c.m.}}/V \gtrsim 1.10$. We conclude that the relative values of σ_R for $E_{\text{c.m.}}/V \gtrsim 1.10$ are quite reliable.

TABLE III. Calculated total reaction cross sections.

$E_{\text{c.m.}}/V$	$\sigma_R/\pi R^2$ Square well[a]	Classical[b]
0.98	0.022	0.000
1.00	0.030	0.000
1.05	0.054	0.048
1.10	0.084	0.091
1.15	0.116	0.130
1.20	0.146	0.167
1.25	0.175	0.200
1.30	0.201	0.231
1.40	0.249	0.286
1.50	0.292	0.333
1.60	0.333	0.375
1.70	0.375	0.412
1.80	0.412	0.445
2.00	0.455	0.500
2.20	0.495	0.545
2.40	0.532	0.583

[a] See Ref. 9.
[b] Eq. (11) in text.

We have drawn a single curve in Fig. 2 for all projectiles and targets, namely

$$f_n = (\tfrac{1}{2})^{(E-35)/65}, \quad \text{for} \quad 45<E<120\ \text{MeV}. \quad (12)$$

This equation fits the measurements for all systems within the experimental errors, with the exception of the reactions of Ba^{138} with Ne^{22}. This system gives rise to larger excitation energies and angular momenta than any other system studied.

We conclude that a very substantial fraction of the total cross section leads to (HI,xn)Dy reactions. Also the variations (other than those due to energy) between different projectiles (except Ne^{22}) are probably less than approx. 10%. Note that for the calculation of the average excitation energy $\langle E\rangle_x$, errors in f_n and σ_R tend to compensate.

C. Values of the Average Excitation Energy $\langle E\rangle_x$ for (HI,xn) Reactions

In Sec. III we have defined the average excitation energy $\langle E\rangle_x$ and discussed the relationship of this quantity to the average energy $\langle \epsilon_1\rangle$ associated with the first neutron. The value of $\langle E\rangle_x$ is determined by the ratio of two integrals over excitation energy, as given in Sec. III

$$\langle E\rangle_x = \int_0^\infty (E)F_x(E)dE \Big/ \int_0^\infty F_x(E)dE. \quad (13)$$

A graph of a typical pair of these integrands is shown in Fig. 3. The integrations were performed graphically with a planimeter. Values of $\langle E\rangle_x$ have been determined for 29 reactions of type (HI,xn)Dy^{149}, (HI,xn)Dy^{150}, or (HI,xn)Dy^{151}. Data for the other reactions studied are not extensive enough to obtain values for $\langle E\rangle_x$. The

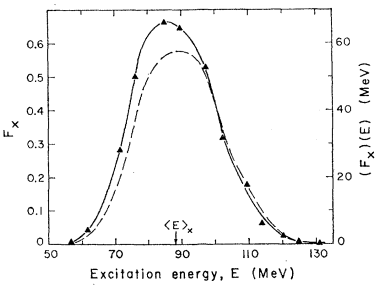

FIG. 3. F_x (solid curve) and (F_x) (E) (dashed curve) versus excitation energy for the reaction Ba^{136} (Ne^{20},6n)Dy^{150}. The value of $\langle E\rangle_x$ is indicated.

results are given in Table IV. Cross-section data in Table II were used with f_n values from Eq. (12) and σ_R values from Table III (column 2). The first column gives the reaction, the second the value of $\langle E\rangle_x$. In the third column is given $\langle E\rangle_x - \sum_{i=1}^{x} B_i$, where B_i is the separation energy of the ith neutron.

It is important to remember that only relative values of (a) the measured cross sections, (b) the product $f_n\sigma_R$, and (c) the masses are important for the determination of the relative values of the average excitation energy $\langle E\rangle_x$. We are interested in the differences between values of $\langle E\rangle_x$, and therefore relative values are of much more concern than the absolute values. Masses of target and Dy nuclei were taken from Seeger's mass formula.[11] The absolute values of the atomic masses from Seeger's Cameron's, and Levy's formulas may differ by several MeV[11–13] but the relative values agree to about 0.5 MeV. A major source of error in the relative values of $\langle E\rangle_x - \sum_{i=1}^{x} B_i$ may be the day-to-day variation in initial energy of the beam from the Hilac. There has been no detailed study of this question, but we estimate a standard error of about ± 1 MeV for the relative values of $\langle E\rangle_x$. In the last column of Table IV is given the average angular momentum $\langle J\rangle$ that corresponds to each value of $\langle E\rangle_x$. These values have been calculated from the sharp cutoff approximation,

$$\langle J\rangle = \frac{(8\mu)^{1/2}R(E_{\text{c.m.}}-V)^{1/2}}{3\hbar}, \tag{14}$$

where μ is the reduced mass, and R is the sum of the radii (radius parameter 1.5 F) of the collision partners [see Eq. (19)].

The values of $\langle E\rangle_x - \sum_{i=1}^{x} B_i$ are plotted against average angular momentum $\langle J\rangle$ in Fig. 4. From the data for reactions with neutron number x ranging from 4 to 9, we can establish that increasing angular momentum $\langle J\rangle$ increases $\langle E\rangle_x - \sum_{i=1}^{x} B_i$. This increase probably reflects an increase in total photon energy with angular momentum. A linear dependence of $\langle E\rangle_x - \sum_{i=1}^{x} B_i$ on $\langle J\rangle$ with slope $+0.47\pm 0.2$ MeV is consistent with all the data.

In order to use Eq. (9) of Sec. III to extract the average energy associated with the first neutron, we must know the average change ΔJ_1 in angular momen-

TABLE IV. Average energies and angular momenta.

Reaction	$\langle E\rangle_x$ (MeV)	$\langle E\rangle_x - \sum_{i=1}^{x} B_i$ (MeV)	$\langle J\rangle$
$Nd^{142}(C^{12},3n)Dy^{151}$	45.4	18.7	21.1
$Nd^{142}(C^{12},4n)Dy^{150}$	59.8	25.2	29.5
$Nd^{142}(C^{12},5n)Dy^{149}$	75.6	30.8	36.7
$Pr^{141}(N^{14},4n)Dy^{151}$	54.0	20.2	23.6
$Pr^{141}(N^{14},5n)Dy^{150}$	70.2	28.5	33.7
$Pr^{141}(N^{14},6n)Dy^{149}$	86.1	34.2	41.3
$Nd^{144}(C^{12},5n)Dy^{151}$	68.6	25.8	33.1
$Nd^{144}(C^{12},6n)Dy^{150}$	85.2	34.5	40.0
$Pr^{141}(N^{15},6n)Dy^{150}$	85.5	34.8	43.6
$Pr^{141}(N^{15},7n)Dy^{149}$	100.8	39.9	49.9
$Ce^{140}(O^{16},5n)Dy^{151}$	71.4	28.6	38.5
$Ce^{140}(O^{16},6n)Dy^{150}$	87.2	36.5	46.2
$Ce^{140}(O^{16},7n)Dy^{149}$	102.3	41.4	52.5
$Ba^{136}(Ne^{20},5n)Dy^{151}$	73.0	30.2	39.5
$Ba^{136}(Ne^{20},6n)Dy^{150}$	88.0	37.3	48.4
$Ba^{136}(Ne^{20},7n)Dy^{149}$	102.5	41.6	55.6
$Ba^{137}(Ne^{20},6n)Dy^{151}$	88.2	38.6	48.5
$Ba^{137}(Ne^{20},7n)Dy^{150}$	101.9	44.4	55.4
$Ba^{137}(Ne^{20},8n)Dy^{149}$	116.9	49.2	62.0
$Ce^{140}(O^{18},7n)Dy^{151}$	100.4	42.1	54.2
$La^{139}(F^{19},7n)Dy^{151}$	99.8	41.5	52.9
$La^{139}(F^{19},8n)Dy^{150}$	114.5	48.3	59.4
$La^{139}(F^{19},9n)Dy^{149}$	129.0	52.6	65.2
$Ba^{138}(Ne^{20},7n)Dy^{151}$	100.1	41.8	54.6
$Ba^{138}(Ne^{20},8n)Dy^{150}$	115.5	49.3	61.5
$Ba^{138}(Ne^{20},9n)Dy^{149}$	129.4	53.0	67.2
$Ba^{137}(Ne^{22},8n)Dy^{151}$	116.9	52.1	66.0
$Ba^{137}(Ne^{22},9n)Dy^{150}$	131.0	58.3	72.0
$Ba^{138}(Ne^{22},9n)Dy^{151}$	128.7	55.6	71.5

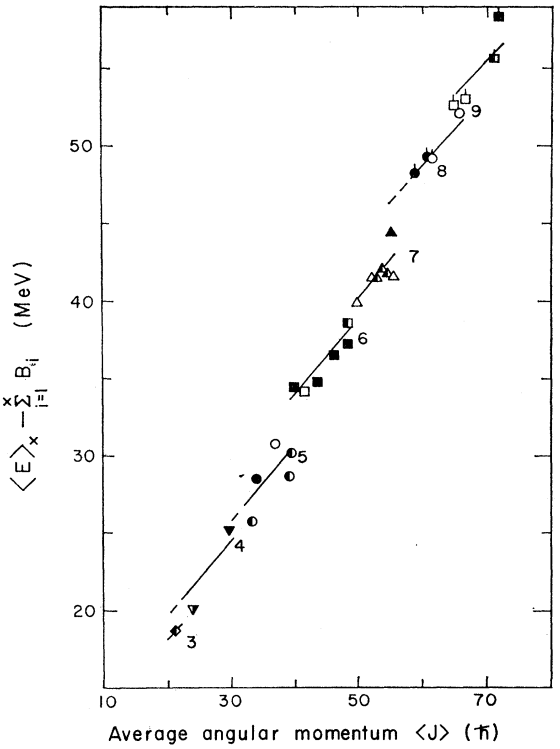

FIG. 4. The average excitation energy $\langle E\rangle_x$ minus the sum of the binding energies B_i of the neutrons as a function of the average angular momentum $\langle J\rangle$. Different symbols are used for the (HI,xn) reactions with the different x values indicated. Open points are for Dy^{149}; closed for Dy^{150}; and half open for Dy^{151}.

[11] P. A. Seeger, Nucl. Phys. **25**, 1 (1961).
[12] A. G. W. Cameron, Atomic Energy of Canada Limited Report CRP-690, 1957 (unpublished).
[13] J. Riddell, Atomic Energy of Canada Limited Report CRP-654, 1956 (unpublished).

TABLE V. Average energy of the first emitted neutron $\langle k_1\rangle$ in (HI,xn)Dy reactions.

x	$\langle k_1\rangle$(MeV) Angular distribution[a]	Cross sections[b]	Ratio
4	3.4±0.3	1.8±1.8	0.53±0.53
5	3.8±0.4	1.6±1.5	0.42±0.42
6	4.2±0.4	3.4±1.5	0.81±0.38
7	4.5±0.5	1.6±1.5	0.36±0.36
8	4.8±0.5	3.9±1.5	0.81±0.33
9	5.1±0.5	2.2±1.5	0.43±0.29
av	4.3	2.4	0.56

[a] Eq. (16).
[b] Eq. (15).

tum due to the emission of the first neutron. Pik-Pichak has calculated $\Delta J_1\approx\frac{1}{2}$ for a nucleus of mass 50 having the moment of inertia of a rigid sphere, and angular momentum and excitation energy comparable to the Dy nuclei formed in this study.[14] Thomas has obtained a similar result for a nucleus of mass 209.[15] If no photons accompany the first neutron and if $\Delta J_1=\frac{1}{2}$, we have

$$\langle\epsilon_1\rangle=\langle k_1\rangle=d_x+0.23\,\text{MeV}, \tag{15}$$

where d_x is the displacement between the lines for (HI,xn) and [HI, $(x-1)n$] reactions. [If photons accompany the first neutron then $\langle k_1\rangle<\langle\epsilon_1\rangle$.] The placement of each line is uncertain by about ±1 MeV and the extrapolation of several of the lines leads to additional uncertainty. We can expect an over-all standard error of about ±1.5 MeV in the values of d_x.

The value of the average neutron energy $\langle k_1\rangle$ can also be inferred from angular-distribution measurements.[3] A comparison of the neutron energies from the two independent studies is interesting. Angular-distribution data have been used to obtain the average total energy (T_n) of the neutrons. These average total energies of the neutrons are approximately proportional to the square root of the excitation energy or to the square root of neutron number x. It is therefore reasonable to expect that the average energy of the first neutron $\langle k_1\rangle$ will also be proportional to $\sqrt{x}$. Using the results of Ref. 3 to obtain the proportionality constant, we have

$$\langle k_1\rangle=1.7\sqrt{x}\,\text{MeV}. \tag{16}$$

The evaluation of $\langle k_1\rangle/\sqrt{x}$ was made at the excitation energy $\langle E\rangle_x$ for each reaction. Experimental sources give rise to errors of about ±10% in the proportionality constant 1.7 MeV. The assumption of isotropic emission of neutrons, if in error, makes the values of the neutron energy $\langle k_1\rangle$ from Eq. (16) too small.[3]

In Table V we list the values of the average energy of the first neutron $\langle k_1\rangle$ from Eqs. (15) and (16). Also we give the ratio. Even though the uncertainties are rather large, it is interesting that all values derived from excitation functions are smaller than those from angular distributions. This discrepancy is even more pronounced if the initial photon energy $\langle\gamma_1\rangle$ is appreciable. It is certainly possible that there is some systematic error of which we are not aware. One possibility is that the lines of Fig. 4 have a slope ≈0.2 MeV rather than 0.47 MeV. This would require that the errors in $\langle E\rangle_x-\sum_{i=1}^{x}B_i$ be somewhat larger than we estimate.

Another possibility is that the change in angular momentum ΔJ_1 has been estimated incorrectly. If ΔJ_1 were 3, then Eq. (15) would read

$$\langle k_1\rangle=d_x+(1.4\pm0.6)\,\text{MeV}. \tag{17}$$

In this case there would be a greater degree of consistency between analyses of excitation functions and angular distribution. Preliminary calculations by Thomas[15] indicate that a moment of inertia (appropriate to the nuclear level density) of about $\frac{1}{4}$ that of a rigid sphere is required to give this result ($\Delta J_1=3$). Theoretical arguments have been given to show that the appropriate moment of inertia is not expected to be less than that of a rigid sphere.[14,16] Additional experimental evidence is certainly required to determine how much angular momentum is taken away by the neutrons. However, these results seem to suggest that $\Delta J_1\approx3$ compared to theoretical estimates of $\Delta J_1\approx\frac{1}{2}$. If the change in angular momentum is actually as large as suggested ($\Delta J_1\approx3$), then the orbital angular momentum of each neutron must be essentially parallel to that of the compound nucleus.

From the values of the average excitation energy $\langle E\rangle_x$ it is possible to obtain the relationship between average total photon energy and average total angular momentum removed by photons. Using Eq. (16) as the most reliable estimate of average neutron energy, we can subtract from each value of the average excitation energy $\langle E\rangle_x$ the sum of the binding and average kinetic energies of each neutron. The remaining energy $\langle T_\gamma\rangle$ must be dissipated by photons. Similarly, we must subtract from the value of the average initial angular momentum $\langle J\rangle$ the sum of the angular momenta removed by the neutrons. In the preceding paragraph we gave evidence that suggested rather large changes in angular momentum for each emitted neutron ($\Delta J_1\approx3$). Let us consider the classical approximation for the average orbital angular momentum l_n of a neutron of energy $\langle k_1\rangle$. If the directions of these angular momenta l_n are parallel to J, then we have

$$l_n=\Delta J_1\approx\frac{\mu^{1/2}R_c\langle k_1\rangle^{1/2}}{\hbar}, \tag{18}$$

where R_c is the radius of the emitting nucleus. This re-

[14] G. A. Pik-Pichak, Zh Eksperim. i Teor. Fiz. **38**, 768 (1960) [translation: Soviet Physics—JETP **11**, 557 (1960)].
[15] T. D. Thomas, Princeton University, 1962 (private communication).
[16] H. Bethe, Rev. Mod. Phys. **9**, 69 (1937); C. Bloch, Phys. Rev. **93**, 1094 (1954).

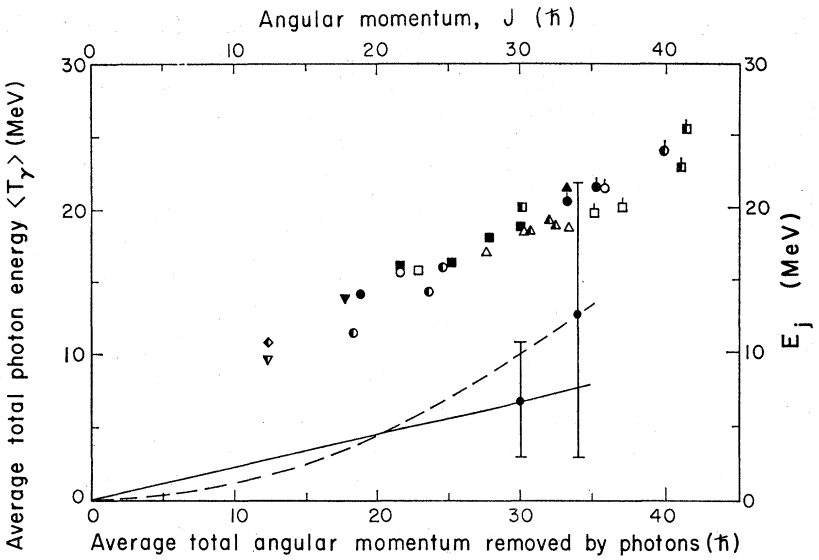

FIG. 5. Average total photon energy $\langle T_\gamma \rangle$ versus average total angular momentum removed by the photons. Symbols are as in Fig. 4. Also indicated is the relationship between E_j and J. The solid line was obtained with the assumption $E_j = c_1 J$; the dashed line with $E_j = c_2 J^2$.

lationship combined with Eq. (16) leads to ΔJ_1 values of 2 to 4. If we subtract from the values of the average initial angular momentum $\langle J \rangle$ the values of ΔJ from Eq. (18) (for each successive neutron), we might expect to arrive at a lower limit for the angular momentum removed by photons. However, there is evidence that the values of $\langle J \rangle$ from Eq. (14) probably overestimate the average angular momenta of the compound nuclei.[1,17] Noncompound nucleus reactions occur and probably deplete the number of compound nuclei of higher spins. Therefore, since these errors tend to cancel, the use of Eq. (14) for $\langle J \rangle$ and Eq. (18) for ΔJ probably leads to a reasonable estimate for the total average angular momentum removed by photons.

In Fig. 5 we show the results obtained by the procedure just described. Note that each experimental point in Fig. 5 was obtained from values of the average excitation energy and angular momentum ($\langle E \rangle_x$ and $\langle J \rangle$). Therefore each point represents an average over all energies for a given reaction. (Roughly speaking, each point is from the peak of an excitation function.) There are several interesting features of this graph. First, all the different measurements from reactions of neutron number (x) 3 to 9 give a consistent trend—namely, a roughly linear increase of total photon energy $\langle T_\gamma \rangle$ with average angular momentum. Second, the slope of the line is 0.46 ± 0.15 MeV/$\hbar$—essentially the same as that in Fig. 4. Combining Fig. 5 with Mollenauer's measurement of 1.2 ± 0.3 MeV per photon,[5] we obtain an average of $1.8 \pm 0.6\hbar$ for the angular momentum removed by each photon. This result is in accord with the number of photons per reaction that Mollenauer observed for Te+C^{12}. But it is surprising that Mollenauer's relative photon yields at 45 and 90 deg (for Te+C^{12}) indicated dipole radiation.[5]

The plot shown in Fig. 5 is, of course, intimately related to the dependence of E_j (the energy of the lowest state of spin J) on J. For each J, the total photon energy $\langle T_\gamma \rangle$ must be greater than the energy E_j by approximately the separation energy of a neutron.[4] Therefore, the dependence of E_j on J can be inferred from the trend of the points in Fig. 5. An independent estimate of the dependence of E_j on J is given in the next section.

Throughout this discussion we have assumed that in the first step of the evaporation chain essentially no energy is dissipated by photon emission—that is $\langle \gamma_1 \rangle \approx 0$. There is no direct evidence that this assumption is strictly correct. However, the cross-section and angular-distribution results do indicate that the photon energy $\langle \gamma_1 \rangle$ associated with the first neutron decreases with increasing number (x) of emitted neutrons. This conclusion is based on two results: (a) The values of the quantity $(\langle E \rangle_x - \sum_{i=1}^{x} B_i)/x$ are all 5.0 to 6.5 MeV per neutron and do not show a trend that increases with x, and (b) the values of the average neutron energy (T_n/x) do increase with x.[3] From the latter result we infer that the kinetic energy of the first neutron $\langle k_1 \rangle$ increases with x [see Eq. (16)]. The comparison of the two results gives evidence that the ratio $\langle k_1 \rangle / \langle \gamma_1 \rangle$ increases with x.

D. An Estimation of the Dependence of E_j on J

A complete analysis of the results presented here requires a rather difficult calculation. One must consider the distribution in angular momentum of the initial compound nuclei. Then the distributions in energy, angular momentum, and type of emitted particle must be considered for each step of the evaporation chain. Such a calculation is beyond the scope of

[17] V. E. Viola, Jr., T. D. Thomas, and G. T. Seaborg, University of California, Radiation Laboratory—10248, 1962 (unpublished). R. Kaufmann and R. Wolfgang, Phys. Rev. **121**, 192, 206 (1961); J. A. McIntyre, T. L. Watts, and F. C. Jobes Phys. Rev. **119**, 1331 (1960).

this paper. However, with a number of simplifying assumptions and approximations we can arrive at an estimate of the dependence of E_j on J. The essential features of this analysis were suggested to us by Dr. Grover of Brookhaven National Laboratory.

The assumptions made are: (a) The distribution function $P(J)$ that describes the initial spectrum of angular momenta is given by the sharp-cutoff approximation

$$P(J)dJ=(2J/J_{\max}{}^2)dJ \quad \text{for} \quad J<J_{\max}, \tag{19}$$

$$P(J)dJ=0 \quad \text{for} \quad J>J_{\max}, \tag{20}$$

and

$$J_{\max}{}^2=2\mu(E_{\text{c.m.}}-V)R^2\hbar^{-2}. \tag{21}$$

(b) There are only small changes in $P(J)$ as a result of the evaporation of neutrons. (c) The distribution of the total energy T_n of x neutrons is represented

$$P(T_n)dT_n=\frac{1}{(2x-1)!\tau^{2x}}T_n{}^{2x-1}\exp(-T_n/\tau)dT_n, \tag{22}$$

where τ is a nuclear temperature parameter. This expression originates from the constant-nuclear-temperature approximation developed by Jackson.[18] In this approximation $T_n/x=2\tau$. Thus, we obtain a value of τ for each value of E from the T_n values given in Ref. 3.

(d) The dependence of E_j on J is given by

$$E_j=c_1J, \tag{23}$$

or

$$E_j=c_2J^2, \tag{24}$$

and (e) neutron emission takes place if the excitation energy exceeds the sum of E_j and the separation energy of a neutron. The physical consequences of this assumption are described by a very illustrative graphical representation in Ref. 4.

We shall develop an approximate relationship between the constants c_1 or c_2 and the values of fractional cross sections F_x for the reactions (HI,xn) [(see Eq. (1)]. Let us consider initial excitation energies 10 to 30 MeV less than $\langle E\rangle_{x+1}$—in other words, the leading edge of the excitation function for the reaction [HI,$(x+1)n$].

After the emission of x neutrons, we require assumption (e), above, that another neutron will be emitted only if

$$M_x-T_n>E_j+B_{x+1}, \tag{25}$$

where

$$M_x=E-\sum_{i=1}^{x}B_i, \tag{26}$$

and B_i is the separation energy of the ith neutron. Then we have

$$\frac{F_{x+1}}{F_x+F_{x+1}}=\frac{\dfrac{1}{(2x-1)!}\displaystyle\int_0^{Jc}J\int_0^{M_{x+1}/\tau}\left(\frac{T_n}{\tau}\right)^{2x-1}\exp\left(-\frac{T_n}{\tau}\right)d\left(\frac{T_n}{\tau}\right)dJ}{\dfrac{1}{(2x-1)!}\displaystyle\int_0^{Jx}J\int_0^{M_x/\tau}\left(\frac{T_n}{\tau}\right)^{2x-1}\exp\left(-\frac{T_n}{\tau}\right)d\left(\frac{T_n}{\tau}\right)dJ}. \tag{27}$$

The limit J_c is obtained from Eq. (23) or (24) and Eq. (25). Hence,

$$J_c=(M_{x+1}-T_n)/c_1 \tag{28}$$

or

$$J_c{}^2=(M_{x+1}-T_n)/c_2. \tag{29}$$

Expressions similar to Eqs. (28) and (29) can be written for the limit J_x, which, with these assumptions, determines the division between the reactions (HI,xn) and [HI, $(x-1)n$]. The accuracy of Eq. (27) depends on the expressions for J_c and J_x which in turn depend strongly on assumption (b), namely that $P(J)$ is essentially unchanged by the evaporation of neutrons. We expect that this assumption is reasonable for the smaller J values[6] (e.g., $J<25$), but it may be very poor for the higher values of J. (See the discussion in the preceding section.) Therefore we confine this treatment to a portion of the leading edge of the excitation function for the [HI, $(x+1)n$] reaction. In this region, typical values of F_{x+1} range from about 0.02 to 0.25, F_x is about 0.5, and F_{x-1} ranges from about 0.4 to 0.2. Therefore, values of J_c are not very large ($J_c<25$), and the values of J_x approach $J_{\max}$. In this energy region we do not lean very heavily on assumption (b) for the higher J values because the value of J_x is not critical.

For simplicity we eliminate J_x from the formulation by the following approximation. In the denominator of Eq. (27) we extend the integration over J from the limit J_x to $J_{\max}$, and we extend the integration over T_n from M_x to ∞. These new limits make a small additional contribution to the integral; this addition depends on initial energy E approximately as does F_{x-1}. With these considerations we change Eq. (27) to read

$$F_{x+1}\approx\frac{F_{x+1}}{F_{x-1}+F_x+F_{x+1}}\approx\frac{\dfrac{1}{(2x-1)!}\displaystyle\int_0^{Jc}J\int_0^{M_{x+1}/\tau}\left(\frac{T_n}{\tau}\right)^{2x-1}\exp\left(-\frac{T_n}{\tau}\right)d\left(\frac{T_n}{\tau}\right)dJ}{\dfrac{1}{(2x-1)!}\displaystyle\int_0^{J\max}J\int_0^{\infty}\left(\frac{T_n}{\tau}\right)^{2x-1}\exp\left(-\frac{T_n}{\tau}\right)d\left(\frac{T_n}{\tau}\right)dJ}. \tag{30}$$

[18] J. D. Jackson, Can J. Phys. **34**, 767 (1956).

The denominator of Eq. (30) is simply $J_{\max}^2/2$, and the numerator can be expressed in the terms of the incomplete gamma function

$$\Gamma_v(p+1)=\int_0^v e^{-x}x^p dx. \tag{31}$$

Integrating and solving for c_1 or c_2, we obtain

$$c_1^2=\frac{1}{F_{x+1}J_{\max}^2}\left[\frac{M_{x+1}^2}{(2x-1)!}\Gamma_{M_{x+1}\tau^{-1}}(2x)-\frac{2M_{x+1}\tau}{(2x-1)!}\Gamma_{M_{x+1}\tau^{-1}}(2x+1)+\frac{\tau^2}{(2x-1)!}\Gamma_{M_{x+1}\tau^{-1}}(2x+2)\right], \tag{32}$$

or

$$c_2=\frac{1}{F_{x+1}J_{\max}^2}\left[\frac{M_{x+1}}{(2x-1)!}\Gamma_{M_{x+1}\tau^{-1}}(2x)-\frac{\tau}{(2x-1)!}\Gamma_{M_{x+1}\tau^{-1}}(2x+1)\right]. \tag{33}$$

One cannot expect this treatment to be very accurate. We can expect only to obtain the trend of the E_j values within about a factor of two.

The application of Eq. (32) yields values of c_1 from 0.10 to 0.36 MeV. Values of c_2 from Eq. (33) range from 0.0025 to 0.019 MeV. The former result is indicated in Fig. 5 by the solid line, the latter result by the dashed line. Both the dashed and the solid lines are consistent with the trend indicated by the values of $\langle T_\gamma\rangle$ shown in Fig. 5. As stated previously, the average total photon energy $\langle T_\gamma\rangle$ is expected to be greater than E_j by about the separation energy of the neutron. This consistency is noteworthy because the approximations made are quite different in the two analyses. The variation in c_1 and c_2 values is large enough that there is a considerable region of overlap of these two representations ($E_j=c_1J$ or $E_j=c_2J^2$).

We might expect a "cold" spinning nucleus to give a reasonable model of the states of highest angular momentum for a given excitation energy. If the cold nucleus has the moment of inertia of a rigid sphere of radius $1.2A^{1/3}$ F, then Eq. (24) is appropriate with a c_2 value of 0.0053 MeV. This model is not inconsistent with the approximate analyses presented above.

V. CONCLUSION

A large body of cross-section data has been presented for reactions of type (HI,xn)Dy^{149}, (HI,xn)Dy^{150}, (HI,xn)Dy^{151}. The fraction of the total reaction cross section that leads to these reactions varies with initial excitation energy from about 0.9 at 45 MeV to about 0.4 at 120 MeV. An analysis of the "first moment" of the excitation functions has been presented. This analysis of the cross-section data leads to estimates of the energy of the first emitted neutron. These energies are consistently smaller than estimates obtained from angular-distribution studies. The discrepancy suggests that the first neutron may remove rather large amounts of angular momentum (2 to 4$\hbar$). A relationship has been obtained between average total photon energy and average total angular momentum removed by the photons. This relationship implies that the average angular momentum removed by each photon is $1.8\pm0.6\hbar$. The dependence of E_j on J has been roughly estimated from the cross-section data.

ACKNOWLEDGMENTS

We thank R. D. Macfarlane for fruitful suggestions and for making available his unpublished data. The crew of the Hilac was very cooperative. We appreciate suggestions from and arguments with J. R. Grover and J. M. Miller. For critical reading of the manuscript we thank E. K. Hyde.